Bound Waves and Sea-Surface Slopes

William J. Plant

Applied Physics Laboratory
University of Washington
1013 NE 40th St
Seattle, WA 98105-6698
plant@apl.washington.edu

Abstract – **For several years, suggestions have been made that sea surface roughness cannot be adequately explained in terms of weakly interacting, wind-generated waves. Rather, ripples that are generated by longer waves, are tilted by them, and are moving at nearly the speed of the longer wave have been postulated to coexist with waves that are directly generated by the wind, that is, with free waves. Effects of these bound waves have been detected in microwave backscatter on the ocean and in wind-wave tanks, and in surface-slope probability density functions (PDFs) in wind-wave tanks. Here we show that Cox and Munk's sea-surface slope PDFs are fully consistent with this bound wave/free wave model. From the fits of these PDFs to the model, we conclude that probabilities of finding bound waves are nearly the same in wind-wave tanks and on the ocean, and both are much higher than the probability of observing whitecaps. Variances of both bound and free waves are larger on the ocean than in tanks.**

INTRODUCTION

The standard view of short waves on the ocean is that they are generated directly by the wind, interact weakly with each other, and are advected and modulated in amplitude by longer waves. Here, we will call such waves "free" waves. A variety of recent microwave measurements in wind wave tanks and on the ocean have indicated that this picture may not be complete (Rozenberg et al., 1995; Plant, 1997; Plant et al., 1999a,b). Rather, many features of these measurements can be explained by postulating that another type of short wave must exist on wind-roughened water surfaces that is generated, not directly by the wind, but by longer waves that were themselves generated by the wind. These are "bound" waves in the sense that they travel at nearly the same speed as their parent wave. The most famous bound waves are parasitic capillaries that are generated by short gravity waves and travel at the speed of the short gravity waves, which is the same as their intrinsic phase speed (Cox, 1958; Longuet-Higgins, 1963; Fedorov and Melville, 1998). Other types of bound waves, breaking or crumpling waves, have been noted and they travel much faster than their intrinsic phase speed (Longuet-Higgins, 1992; Duncan, 1994, 1999). This feature is necessary to explain many microwave observations. Effects of bound waves are easily seen in surface wave slope probability density functions (PDFs) measured in wind-wave tanks but have not previously been suggested as an explanation for such PDFs measured at sea (Plant et al., 1999a).

In this paper, we give examples of bound wave effects that have previously been noted in wind-wave tanks and in microwave backscatter from the ocean. We show that the classic measurements of sea-surface slope PDFs by Cox and Munk (1954, 1956) also conform to a bound wave/free wave model. Parameters of bound and free waves such as their probability of occurrence, mean tilt, and variance can be obtained from PDFs in both wind-wave tanks and on the ocean. The main differences are in the variances, which are much larger at sea. The probability of finding bound waves at sea is much larger than the percent coverage of whitecaps (Monahan, 1971). This indicates that microscale breaking or crumpling waves must be the dominant type of bound waves at sea.

BOUND WAVES AND MICROWAVE BACKSCATTER

Perhaps the most striking example of the effect of bound waves on microwave backscatter from the sea is found in Doppler spectra taken at HH (electric field horizontal on transmit and receive) and VV (electric field vertical on transmit and receive) polarizations at high incidence angles. Fig. 2 shows a typical example of these spectra taken at an 80° incidence angle looking into a 7 m/s wind (Plant, 1997). The striking feature of these spectra is their different frequency shifts: HH spectra are shifted to much higher frequencies than VV.

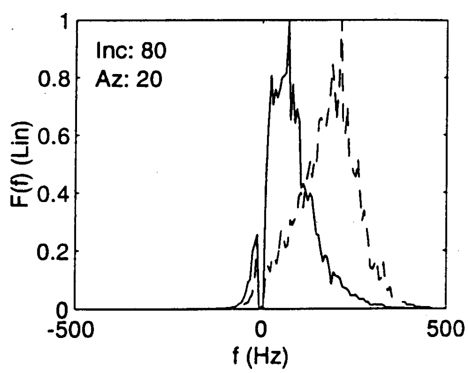

Fig. 1. Normalized 14 GHz Doppler spectra of microwave backscatter from the sea at an 80° incidence angle looking 20° from upwind. Solid = VV, Dashed = HH. Spectra have been set to zero near zero frequency.

The explanation for this different behavior of HH and VV Doppler spectra, offered by Plant (1997), is that Bragg scattering from surface waves falls off much more rapidly with increasing incidence angle for HH backscatter than for VV. Thus the mean tilt of bound waves, on the order of 15^o to 20^o, reduces their local incidence angle when looking into the wind and increases their importance in HH backscatter much more than in VV. Since these bound waves move much faster than their intrinsic phase speed, this accounts for the large Doppler shifts observed in HH spectra.

Similar bound wave effects occur in microwave Doppler spectra observed in wind-wave tanks except that the bound waves in this case are sufficiently energetic that they cause effects at lower incidence angles and for both polarizations. Fig. 2 shows 14 GHz HH and VV Doppler spectra collected in the Canada Centre for Inland Waters (CCIW) wind-wave tank looking upwind at a 45^o incidence angle and a friction velocity of 0.43 m/s. Peaks due to waves bound to the dominant wave in the tank are seen in both spectra while a distinct peak due to free wave is seen only in VV spectra.

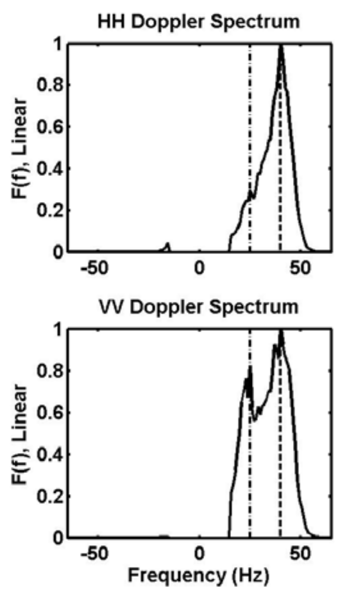

Fig. 2. Normalized 14 GHz Doppler spectra of microwave backscatter in the CCIW wind-wave tank at a 45^o incidence angle looking upwind. The dash-dotted vertical line indicates the expected frequency of free waves. The dashed vertical line shows the expected Doppler shift of bound wave moving at the dominant wave phase speed. Spectra have been set to zero within 15 degrees of zero frequency.

Again, the explanation of the prominance of the peak traveling with the dominant wave is the mean slope of the bound waves riding on the leeward face of the dominant wave. For an antenna directed upwind, this mean tilt decreases the local incidence angle at the location of the bound waves. Since backscatter becomes stronger at smaller local incidence angles, this increases the prominence of the bound waves in the backscatter (Plant et al., 1999a,b).

BOUND WAVES IN SURFACE SLOPE PDFs

If this explanation is indeed correct, then some evidence of ripples tilted at relatively large angles should be present in PDFs of surface slopes. In the CCIW wind-wave tank, a laser slope gauge was operating at the same time that the microwave measurements were made. Fig. 3 shows the PDF of along-tank slopes measured by this gauge at a friction velocity of 0.38 m/s. The protrusion on the negative side of this distribution shows that a high probability indeed exists of finding surface areas whose normal is tilted in the wind direction, as would be the case for ripples on the leeward face of a longer wave. When combined with the microwave evidence that such waves travel at speeds above their intrinsic phase speeds, this feature of the PDF supports the idea that bound waves exist on the surface in addition to free waves.

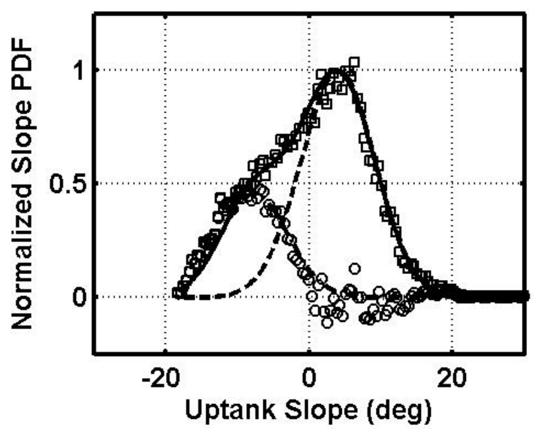

Fig. 3. Normalized surface slope PDF for along-tank slopes in the CCIW wind-wave tank. Squares are measurements, dashed line is a Gaussian fit to points at frequencies above the peak, open circles are the differences between squares and the dashed line, dash-dotted line is a Gaussian fit to the circles, and the solid line is the overall fit to the probability distribution given by (1).

If bound and free waves are statistically independent, then Bayes theorem states that the overall probability distribution, P(s), is given by

$$P(s) = P_f\, P(s|f) + P_b\, P(s|b) \qquad (1)$$

where P_f is the total probability of finding bound waves on the surface, Pb is the total probability of finding free waves and P(s|x) is the conditional PDF of slopes at locations containing free waves (x=f) or bound waves (x=b). The dashed and dash-dotted (hidden by the circles) lines in Fig. 3 are P(s|f) and P(s|b) that best fit the data while the solid line is P(s) obtained from (1).

Probability density functions of sea surface slopes were first reported in the classic sun-glitter measurements of Cox and Munk (1954). An example of their fit of a Gram-Charlier PDF to the measured data is shown as the solid curve in Fig. 4.

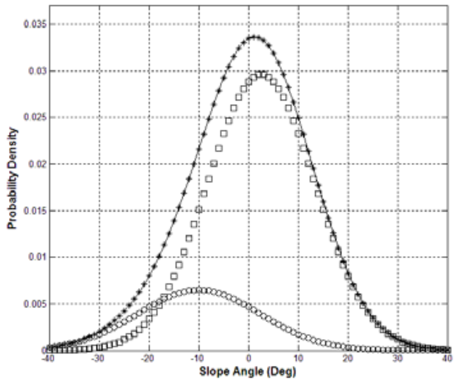

Fig. 4. The solid curve is the best fit of Cox and Munk's (1954) data to a Gram-Charlier probability density function (PDF). The squares are a Gaussian PDF representing free waves while the circles are a Gaussian PDF representing bound waves. The asterisks are the best fit to the solid curve using (1).

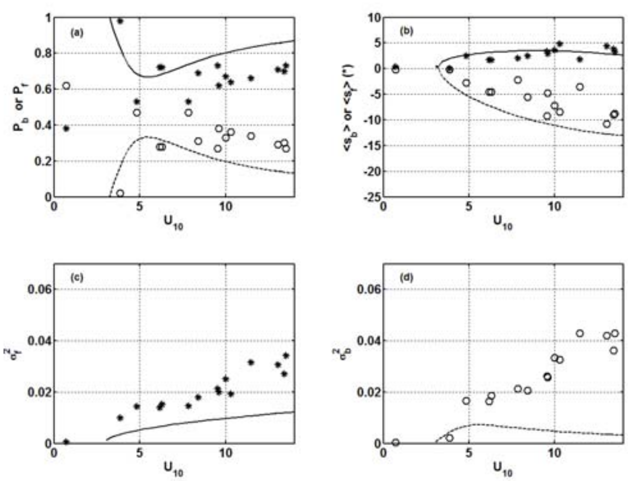

Fig. 5. Bound and free wave parameters versus wind speed at 10 m height. Symbols were deduced from fits to the Cox and Munk (1954, 1956) data and therefore represent ocean data. In parts (a) and (b), asterisks In correspond to free waves and open circles are bound wave values. Solid and dashed curves show best fits to results obtained in a wind-wave tank (Plant et al., 1999a).

Although these PDFs contain no obvious protrusion at large negative values as do PDFs measured in the wind-wave tank, we have found that they also can be well fit by a bound wave/free wave model (Plant, 2003). The Gaussian functions shown by the circles and squares in the figure are $P_bP(s|b)$ and $P_fP(s|f)$, respectively, which yield the best fit to the Gram-Charlier PDF when inserted into (1). This best fit is obtained by minimizing the difference between the solid line and the asterisks while simultaneously minimizing the difference between the fourth moments of the two distributions.

In order to obtain this fit, parameters of the two Gaussian functions were varied. These parameters are P_f and P_b, the mean tilts, $<s_f>$ and $<s_b>$, and the variances σ_f^2 and σ_b^2, where f and b refer to free and bound waves. The values of these parameters obtained by fitting Cox and Munk's data are plotted versus the wind speed at 10 m height in Fig. 5 as the symbols. The curves in this figure show the same parameters determined from fits of the wind-wave tank slope PDFs. Clearly, the probabilities of finding free and bound waves in the wind-wave tank and on the ocean are similar. Furthermore, they are much larger than the ~1% probability of finding whitecaps on the ocean (Monahan, 1971). This indicates that most bound waves do not correspond to breaking waves that entrain air but are more likely to be microbreakers or parasitic capillaries that produce a much weaker visual signature. The mean slopes of free and bound waves are also similar in the tank and on the ocean. It is interesting to note that since the bound waves have negative mean slopes, the free waves must have positive ones in order that the mean tilt of the sea surface be zero. Finally, the variances of both bound and free waves are significantly larger on the ocean than they are in the wind-wave tank. This is the reason that they are more easily recognized in slope PDFs in the tank than they are on the ocean.

REFERENCES

Cox, C.S., Measurements of slopes of high-frequency wind waves, J. Marine Res., 16, 199-225, 1958.

Cox, C. and W. Munk, Statistics of the sea surface derived from sun glitter, J. Mar. Res., 13(2), 199-227, 1954.

Cox, C. and W. Munk, Slopes of the sea surface deduced from photographs of sun glitter, Bull. Scripps Inst. Oceanogr., 6, 401-488, 1956.

Duncan, J.H., V. Philomin, M. Behres, and J. Kimmel, The formation of spilling breaking water waves, Phys. Fluids, 6, 2558-2560, 1994.

Duncan, J.H., H. Qiao, V. Philomin, and A. Wenz, Gentle spilling breakers: crest profile evolution, J. Fluid Mech., 379, 191-222, 1999.

Fedorov, A.W., and W.K. Melville, Nonlinear gravity-capillary waves with forcing and dissipation, J. Fluid Mech., 354, 1-42, 1998.

Longuet-Higgins, M.S., The generation of capillary waves by steep gravity waves, J. Fluid Mech., 16, 138-159, 1963.

Longuet-Higgins, M.S., Capillary rollers and bores, J. Fluid Mech., 240, 659-679, 1992.

Monahan, E.C., Oceanic Whitecaps, J. Phys. Ocean., 1, 139-144, 1971.

Plant, W.J., A model for microwave Doppler sea return at high incidence angles: Bragg scattering from bound, tilted waves, J. Geophys. Res, 102(C9), p.21131-21146, 1997.

Plant, W.J., W.C. Keller, V. Hesany, T. Hara, E. Bock, and M. Donelan, Bound waves and Bragg scattering in a wind wavetank, J. Geophys. Res., 104(C2), 3243-3263, 1999a.

Plant, W.J., P.H. Dahl, and W.C. Keller, Microwave and acoustic scattering from parasitic capillary waves, J. Geophys. Res., **104**, 25,853-25,866, 1999b.

Plant, W.J., A new interpretation of sea-surface slope probability density functions, in press, J. Geophys. Res., 2003.

Rozenberg, A.D., D.C. Quigley, and W.K. Melville, Laboratory study of polarized microwave scattering by surface waves at grazing incidence: Part I – Wind waves, IEEE Trans. Geosci. Rem. Sens., 33(4),1037-1046, 1995.